Spectrally Resolved Approach for Modeling Short Pulse Amplification in Er^{3+}-Doped Fibers

Eldad Yahel, Ortwin Hess, and Amos Hardy, *Fellow, IEEE*

***Abstract*—We study pulse propagation in Er^{3+}-doped fiber amplifiers (EDFA) within the framework of a spectrally resolved pulse rate-propagation equations model. Our model accounts for the effects of gain dispersion, gain saturation, waveguide and chromatic dispersion, and amplified spontaneous emission. This model allows us to approximate the effects of nonlinear resonant dispersion on short pulse amplification in doped fibers, without reverting to the generalized nonlinear Schroedinger equation. Numerical results of the time-dependent power spectrum of the amplified pulse demonstrate subpicosecond pulse propagation in EDFAs.**

***Index Terms*—Erbium (Er), optical fiber amplifiers, optical fiber dispersion, optical pulse amplifiers.**

I. Introduction

RARE-EARTH-DOPED fibers have a broad gain bandwidth which makes them very attractive for the amplification of subpicosecond optical pulses. For such short pulses, nonlinear resonant effects associated with the dopants inversion are an important amplifier design consideration. In particular, the finite gain bandwidth, and gain-induced dispersion, can severely distort short amplified pulses [1]–[4]. Optical pulse propagation in doped optical fibers is mainly considered analytically [5], and in the framework of a generalized nonlinear Schroedinger equation [6]. In modeling the amplified pulse, the pulse bandwidth is assumed to be relatively narrow, and the gain is assumed to have either constant, parabolic, or a Lorentzian lineshape [3]–[6], which does not accurately predict the observed atomic susceptibility of the dopant ions in a glass system [7]. In this contribution, we extend well-established quasi-continuous-wave rate-propagation models of erbium-doped fiber amplifiers (EDFA) [8] to the short pulsed regime. To this end, a transport equation for the coupled pulse spectral components is derived, which accounts for the changes in the distribution of the pulse power along the fiber. In our model, the spectral gain is resolved using experimentally measured cross sections, Taylor expansion is not assumed for the dispersion, and the modeled pulse bandwidth is not restricted to the precondition of a quasi-monochromatic pulse. The model allows us to calculate the time-dependent power spectrum of the pulse, and thus to simultaneously analyze the signal in the time and spectral domains, which is more compliant with the experimentalist's observations. Furthermore, our model includes the effect of spontaneous emission noise on the pulse dynamics [9]. Our approach is limited to pulsewidths of a few hundred femtoseconds, for which we can assume thermal equilibrium of the atomic populations within each Er^{3+} manifold [9]. The new model is employed to demonstrate the effects of dopant dispersion on the amplification of short optical pulses in the technologically important 1.55-μm range wavelengths.

Manuscript received February 23, 2006; revised June 27, 2006. The work of A. Hardy was supported by the Chana and Heinrich Manderman Chair in Optoelectronics at Tel-Aviv University.

E. Yahel and O. Hess are with the Advanced Technology Institute, University of Surrey, Guildford, Surrey GU2 7XH, U.K. (e-mail: E.Yahel@surrey.ac.uk).

A. Hardy is with the Department of Electrical Engineering, Physical Electronics, Tel Aviv University, Tel Aviv 69978, Israel.

Digital Object Identifier 10.1109/LPT.2006.884751

II. Theoretical Model

We consider a single-clad fiber geometry, for which the core supports a single mode. The core is doped with Er^{3+} ions with uniform concentration N_{Er}. The spectral power densities per unit wavelength $P_s(z,t,\lambda)$, representing signal pulse spectral components that are emitted and amplified due to the Er^{3+} ions, propagate in the forward z direction with a wavelength-dependent power filling factor $\Gamma(\lambda)$. The analysis is based on the assumption that the spatial changes in the refractive index are small. Under this condition, the power transport equation can be extended to take into account dispersion through the photons equations of motion [10], as well as the effects of transients in the refractive index on the wavelength of streaming photons [11]. In particular, the following equation can be derived for the rate of change in the spectral power densities per unit wavelength of the propagating pulse (based on [11]):

$$\frac{dP_s}{dz}+\frac{P_s}{c}\frac{\partial n_{\mathrm{eff}}}{\partial t}=[\Gamma(\lambda)\{N_2(z,t)\sigma_{21}(\lambda)-\sigma_{12}(\lambda)N_1(z,t)\}-\alpha(\lambda)]P_s+\Gamma(\lambda)P_0(\lambda)\sigma_{21}(\lambda)N_2(z,t) \quad (1)$$

where $dP_s(z,t,\lambda)/dz \equiv V_g^{-1}\cdot\partial P_s/\partial t+\partial P_s/\partial z+\lambda/c\cdot\partial n_{\mathrm{eff}}/\partial t\cdot\partial P_s/\partial\lambda$, c is the speed of light in vacuum, and $V_g(z,t,\lambda)=[-\lambda^2/c\cdot\partial(n_{\mathrm{eff}}/\lambda)/\partial\lambda]^{-1}$ is the effective group velocity of the pulse spectral component at the vacuum wavelength λ. The effective refractive index $n_{\mathrm{eff}}(z,t,\lambda)$ of the fundamental LP_{01} mode in the core is given by the sum of passive and active index contributions [6]. The passive contribution is given by the effective index of the host fiber. The active contribution is derived, to a good approximation, using the Kramers–Kronig transform of the imaginary part of the Er^{3+} susceptibility [7]. Additional, nonlinear contributions, e.g., due to the intensity dependence of the refractive index, are disregarded in this work, as we limit ourselves to relatively low pulse intensities. The terms $N_2(z,t)$ and $N_1(z,t)$ are the atomic populations of the $^4I_{13/2}$ and $^4I_{15/2}$ Er^{3+} manifolds, respectively. Other terms in (1) are $\sigma_{ij}(\lambda)$ representing wavelength-dependent emission and absorption cross section

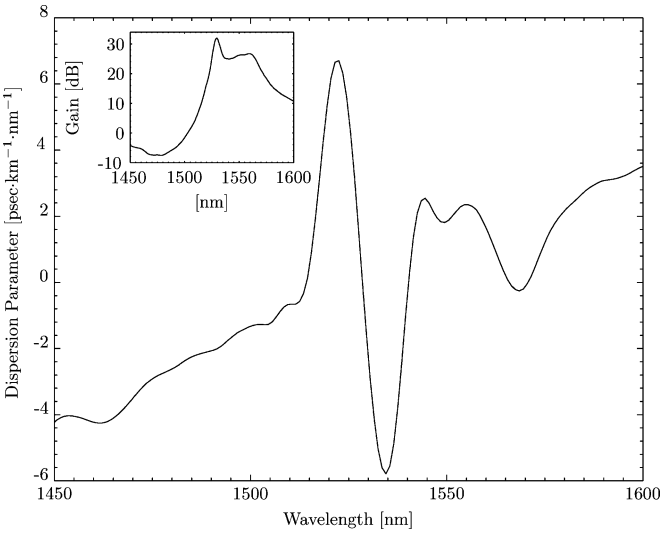

Fig. 1. Dependence of the dispersion parameter (D) on the wavelength. The inset shows the spectrum of the integrated gain (see [12, eq. (14)]).

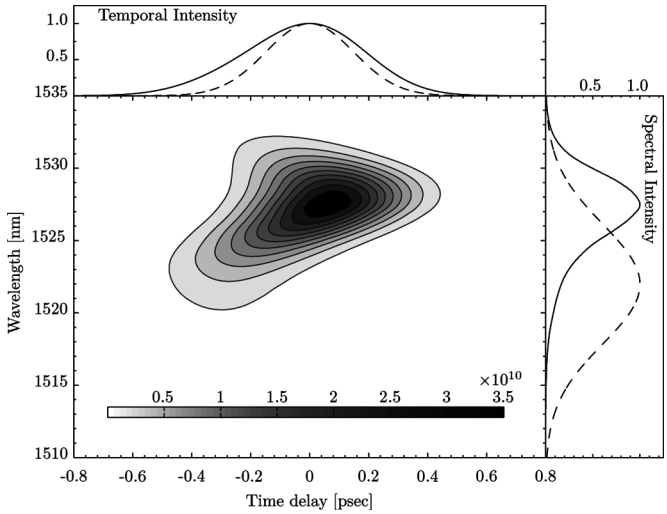

Fig. 2. Contour plot of the pulse intensity (in watts per unit wavelength) at the fiber output, as function of the wavelength and time delay, for an incident pulse around $\lambda_s = 1522$ nm. Darker shades correspond to higher power levels (see inset). Top: temporal intensity, i.e., $\int P_s(z,t,\lambda)d\lambda$ (normalized). Right side: spectral intensity, i.e., $\int P_s(z,t,\lambda)dt$ (normalized). The solid and dashed lines correspond to the intensity distribution of the pulse at $z = L$ and $z = 0$, respectively. The gain in pulse energy is ~24.5 dB.

between levels i and j, and $\alpha(\lambda)$ the fiber scattering loss coefficient. The power density per unit wavelength term $P_0(\lambda)$ represents the contribution of the spontaneous emission into the guided mode [12]. We note that in contrast to the linear power equation that appears in "classical" EDFA theory [8], [9], (1) includes additional terms due to the varying refractive index contributions. Equation (1), coupled with a set of rate equations for the atomic populations of Er^{3+} ions [12], formulate the basis of our spectrally resolved pulse model.

In order to solve (1) numerically, we transform it into a retarded time frame moving with a reference group velocity $V_g^R \simeq c/1.5515$, by defining a reduced time $T \equiv t - z/V_g^R$. Thus, (1) can be written as

$$\frac{\partial P_s}{\partial z} + \left[V_g^{-1} - \left(V_g^R\right)^{-1}\right]\frac{\partial P_s}{\partial T} + \frac{P_s}{c}\frac{\partial n_{\text{eff}}}{\partial T} + \frac{\lambda}{c}\frac{\partial n_{\text{eff}}}{\partial T}\frac{\partial P_s}{\partial \lambda} \simeq [\Gamma(\lambda)\{N_2(z,T)\sigma_{21}(\lambda) - \sigma_{12}(\lambda)N_1(z,T)\} - \alpha(\lambda)]P_s + \Gamma(\lambda)P_0(\lambda)\sigma_{21}(\lambda)N_2(z,T) \quad (2)$$

where the second term on the left-hand side of (2) is due to the dispersion of the pulse spectral components relative to the reference frame.

III. Examples

The parameters that we consider in the numerical calculations correspond to a dispersion-shifted alumino–silicate Er^{3+}-doped fiber. In particular, the Er^{3+} concentration is assumed to be $N_{\text{Er}} = 1.5 \times 10^{25}$ m^{-3}, the core area is $A_{\text{core}} = 1.89 \times 10^{-11}$ m^2, and the numerical aperture is NA $= 0.21$. We also assume a constant input pump power of $P_p = 25$ mW at $\lambda_p \simeq 1.49$ μm and an $L = 5$ m long fiber. Under these assumptions, the gain-induced contribution to the refractive index strongly modifies the fiber dispersion characteristics. Fig. 1 shows the calculated spectrum of the dispersion parameter, i.e., $D = -\lambda/(\text{Lc}) \cdot d^2[\int_0^L n_{\text{eff}}dz]/d\lambda^2$, based on cross section data taken from [13]. Here, the passive fiber contribution includes the waveguide dispersion, and the chromatic dispersion of the host, e.g., as calculated from Sellmeier's equation [14]. We note that due to the Er^{3+} contribution, the dispersion parameter takes both positive and negative values at a spectral range near $\lambda \simeq 1529$ nm.

In what follows, we employ our model in order to analyze short pulse propagation around $\lambda_s = 1522$ nm and $\lambda_s = 1535$ nm, namely in the anomalous and normal dispersion regimes of the fiber (cf. Fig. 1), respectively. We assume that the incident pulse shape is an unchirped Gaussian, centered at $t = 0$ with width (FWHM) of $T_0 \simeq 350$ fs. We further assume that the peak power of the incident pulse is ~1 W, and therefore, saturation effects are small in the present calculations. The distribution of the incident pulse in the hybrid time and wavelength space, i.e., $P_s(z = 0, t, \lambda)$, is calculated using the Wigner distribution function [15]. Thus, the resulting pulse distribution is a transform-limited bell-shaped surface centered at λ_s. It is worth mentioning, however, that the incident pulse can be resolved using other time-frequency distributions that satisfy the physical margins (i.e., energy conservation).

Fig. 2 shows contour plots of the pulse intensity around $\lambda_s = 1522$ nm, after amplification along the EDFA, as function of the wavelength and the time delay relative to the arrival time of the pulse temporal intensity peak. That is, we plot $P_s(z = L, t, \lambda)$. The calculated output pulse intensity is a complex interplay between the dispersion and the wavelength dependence of the gain, and it significantly deviates from the incident Gaussian pulse distribution. In particular, the short spectral components of the pulse acquire negative chirp, i.e., longer wavelengths travel in slower velocities, due to the anomalous dispersion in the EDFA (see Fig. 1). On the other hand, the pulse chirp gradually changes sign in the limit of longer pulse spectral components. This, in turn, broadens the output pulse by approximately $\Delta T_0 \simeq 131$ fs relative to the width of the incident pulse. We note that the peak of the output pulse spectrum is shifted toward longer wavelengths, due to the preferential amplification of pulse spectral

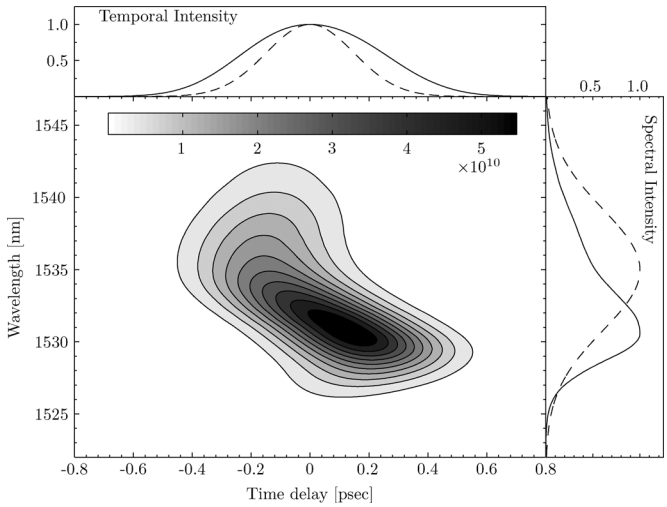

Fig. 3. Same as Fig. 2, but for an incident pulse around $\lambda_s = 1535$ nm. The energy gain is ~27.8 dB.

components near the gain peak ($\lambda \simeq 1530$ nm, see inset of Fig. 1) [6]. We also note that the bandwidth of the output pulse is narrower, in about $\Delta\Lambda \simeq -4.5$ nm, relative to the incident pulse bandwidth. The output pulse intensity distribution shows somewhat different characteristics for a pulse incident around $\lambda_s = 1535$ nm, as illustrated in Fig. 3. Here, the shorter pulse spectral components acquire positive chirp due to propagation in the normal dispersion regime, in agreement with the negative value of D (see Fig. 1). Also the temporal broadening and bandwidth narrowing of the output pulse are $\Delta T_0 \simeq 197$ fs and $\Delta\Lambda \simeq -2.9$ nm, respectively. Furthermore, the output pulse spectrum is strongly asymmetrical due to the gain spectrum, and it is pulled towards the gain peak at shorter wavelengths. We also found that the temporal width of an incident pulse can be decreased, provided that the pulse is initially chirped and the fiber dispersion induces chirp with opposite sign [1]. We conclude that the output pulse spectrogram strongly depends on the relative position of the gain peak wavelength with respect to the incident pulse wavelength.

It is worth noting that our calculated intensity distribution, i.e., the quantity $P_s(z,t,\lambda)$ in (1), can be obtained, to a good approximation, by experimentally measuring the spectrogram of the amplified pulse using a known gate function. For example, using the cross-correlation frequency-resolved optical gating pulse measurement setup [16].

IV. Conclusion

We have analyzed the effects of resonant dispersion due to Er^{3+} ions on subpicosecond pulse propagation in dispersion-shifted EDFA, using a new, spectrally resolved pulse rate-propagation equations model. Our results demonstrate the temporal and spectral characteristics of the amplified pulse. In particular, the output pulse spectrum, chirp, and temporal broadening (or compression) are strongly dependent on the fiber dispersion regime and spectral gain, and hence on the incident pulse wavelength. The mathematical model presented in this work allows us to approximate broad bandwidth pulse propagation in doped optical fibers, without considering the complex field envelope of the pulse. More intense signal pulses, for which nonlinear fiber effects are significant, are the subject of a subsequent publication.

Acknowledgment

E. Yahel would like to thank Dr. R. Z. Yahel for drawing his attention to the works of G. C. Pomraning, and K. Boehringer for some very fruitful discussions.

References

[1] J. M. Dudley, L. P. Barry, P. G. Bollond, J. D. Harvey, and R. Leonhardt, "Characterizing pulse propagation in optical fibers around 1550 nm using frequency-resolved optical gating," *Opt. Fiber Tech.*, vol. 4, pp. 237–265, 1998.

[2] M. Romagnoli, F. S. Locati, F. Matera, M. Settembre, M. Tamburrini, and S. Wabnitz, "Role of pump-induced dispersion on femtosecond soliton amplification in erbium-doped fibers," *Opt. Lett.*, vol. 17, no. 13, pp. 923–925, Jul. 1992.

[3] A. C. Peacock, R. J. Kruhlak, J. D. Harvey, and J. M. Dudley, "Solitary pulse propagation in high gain optical fiber amplifiers with normal group velocity dispersion," *Opt. Commun.*, vol. 206, pp. 171–177, May 2002.

[4] D. B. S. Soh, J. Nilsson, and A. B. Grudinin, "Efficient femtosecond pulse generation using a parabolic amplifier combined with a pulse compressor. ii. finite gain-bandwidth effect," *J. Opt. Soc. Amer. B*, vol. 23, no. 1, pp. 10–19, Jan. 2006.

[5] M. B. Hoffman and J. A. Buck, "Erbium resonance-based dispersion effects on subpicosecond pulse propagation in fiber amplifiers: Analytical studies," *J. Opt. Soc. Amer. B*, vol. 13, no. 9, pp. 2012–2016, Sep. 1996.

[6] G. P. Agrawal, "Optical pulse propagation in doped fiber amplifiers," *Phys. Rev. A*, vol. 44, no. 11, pp. 7493–7501, Dec. 1991.

[7] E. Desurvire, "Study of the complex atomic susceptibility of erbium-doped fiber amplifiers," *J. Lightw. Technol.*, vol. 8, no. 10, pp. 1517–1527, Oct. 1990.

[8] C. R. Giles and E. Desurvire, "Modeling erbium-doped fiber amplifiers," *J. Lightw. Technol.*, vol. 9, no. 2, pp. 271–283, Feb. 1991.

[9] E. Desurvire, *Erbium-Doped Fiber Amplifiers Principles and Applications*, 1st ed. New York: Wiley, 1994.

[10] E. G. Harris, "Radiative transfer in dispersive media," *Phys. Rev.*, vol. 138, no. 2B, pp. 479–485, Apr. 1965.

[11] G. C. Pomraning, "Radiative transfer in dispersive media," *Astrophys. J.*, vol. 153, pp. 321–324, Jul. 1968.

[12] E. Yahel and A. Hardy, "Efficiency optimization of high-power, Er^{3+}-Yb^{3+}-codoped fiber amplifiers for wavelength-division-multiplexing applications," *J. Opt. Soc. Amer. B*, vol. 20, no. 6, pp. 1189–1197, Jun. 2003.

[13] W. L. Barnes, R. I. Laming, E. J. Tarbox, and P. R. Morkel, "Absorption and emission cross section of Er^{3+} doped silica fibers," *IEEE J. Quantum Electron.*, vol. 27, no. 4, pp. 1004–1010, Apr. 1991.

[14] G. Ghosh, M. Endo, and T. Iwasaki, "Temperature-dependent sellmeier coefficients and chromatic dispersions for some optical fiber glasses," *J. Lightw. Technol.*, vol. 12, no. 8, pp. 1338–1342, Aug. 1994.

[15] J. Paye, "The chronocyclic representation of ultrashort light pulses," *IEEE J. Quantum Electron.*, vol. 28, no. 10, pp. 2262–2273, Oct. 1992.

[16] S. Linden, J. Kuhl, and H. Giessen, "Amplitude and phase characterization of weak blue ultrashort pulses by downconversion," *Opt. Lett.*, vol. 24, no. 8, pp. 569–571, Apr. 1999.